

Supplemental Information

3' Uridylation Confers miRNAs With Non-canonical Target Repertoires

Acong Yang, Xavier Bofill-De Ros, Tie-Juan Shao, Minjie Jiang, Katherine Li, Patricia Villanueva, Lisheng Dai, Shuo Gu

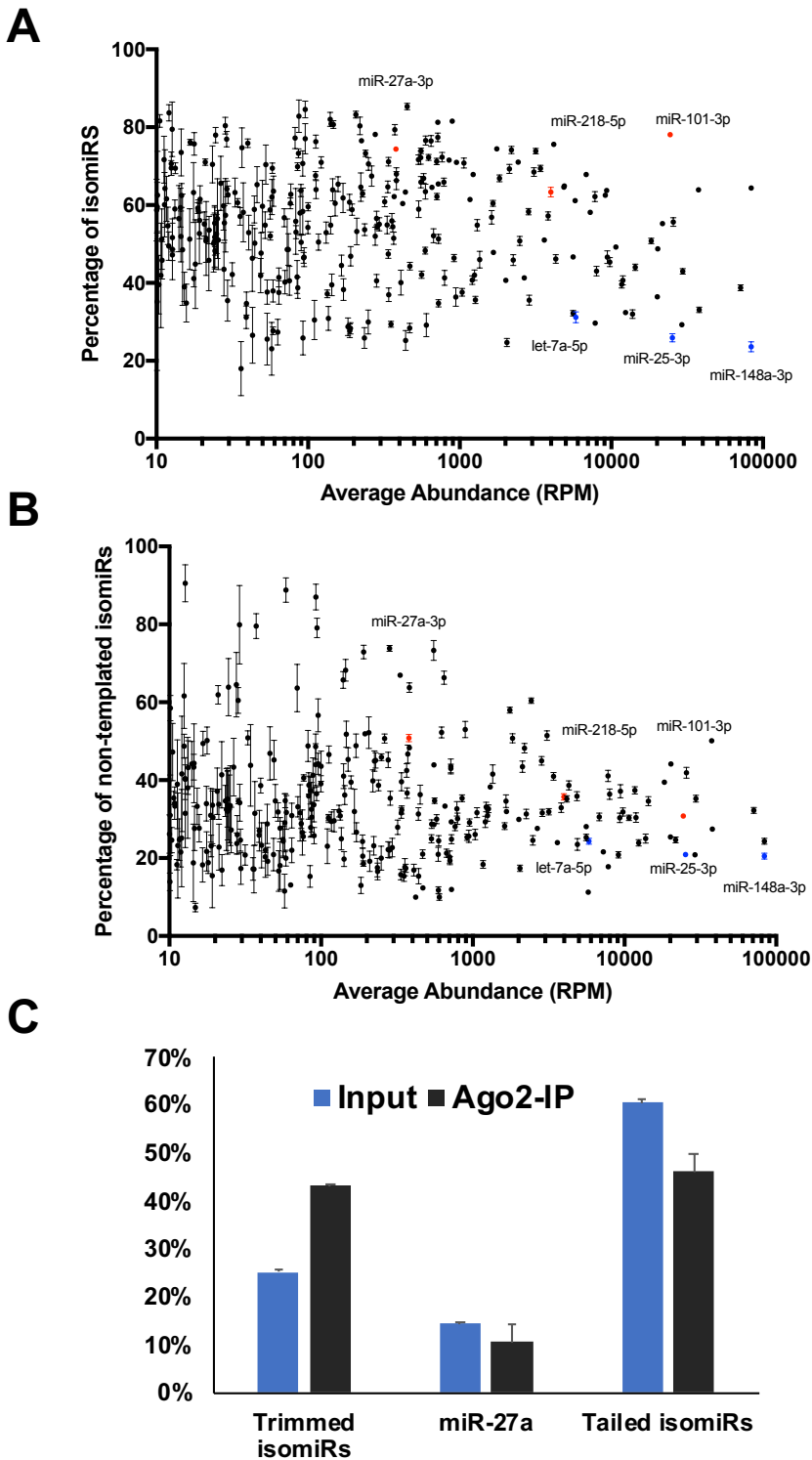
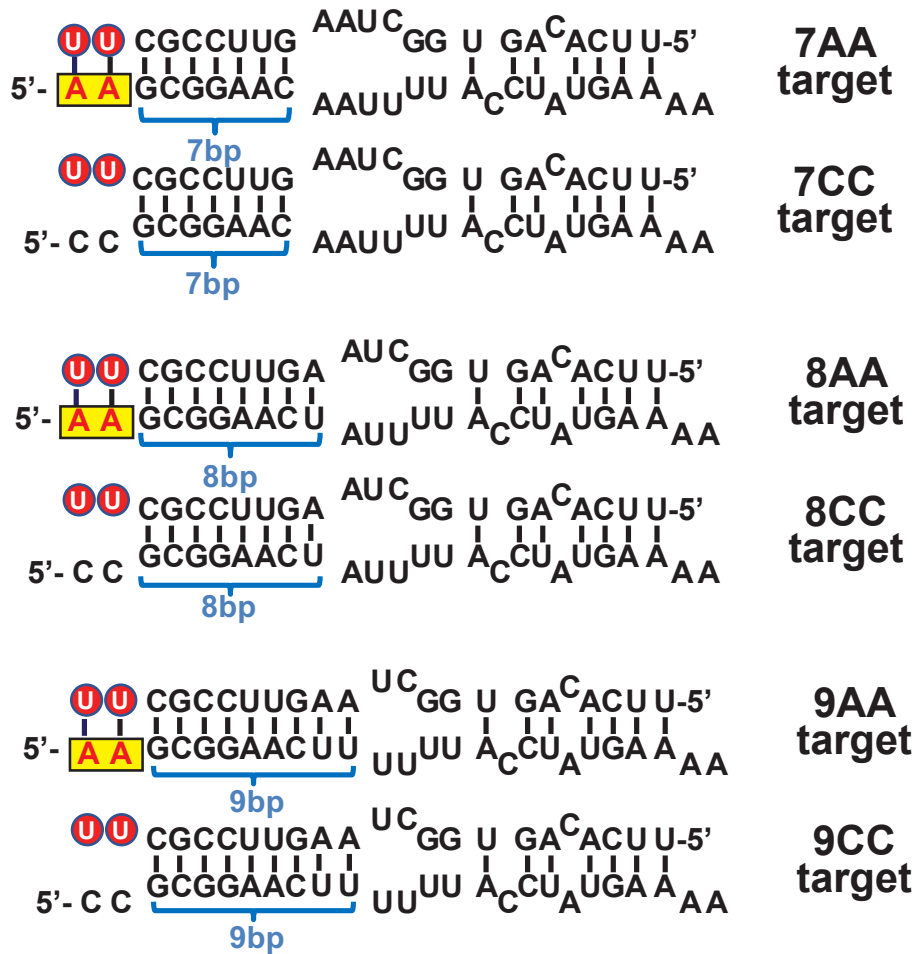
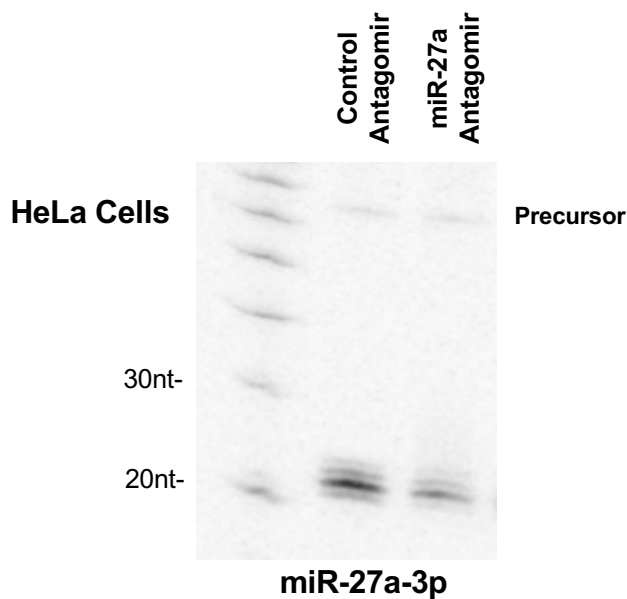


Figure S1. 3' uridylation of isomiRs are associated with RISC. Related to Figure 1.

(A) Small RNAs extracted from HEK293T cells were subjected to deep sequencing. After being mapped to genome sequence, miRNAs and their isomiRs were analyzed. For each miRNA, the most abundant isoform was categorized as the canonical sequence, which in most cases is the same as annotated in the miRBase. The rest of reads were categorized as isomiRs. Deep sequencing of three biological replicates were performed. The average percentage of isomiRs was plotted against the expression level for each miRNA with an average abundance over 10 reads per million (RPM). Error bar indicates the standard deviation ($n=3$). (B) The average percentage of isomiRs resulting from non-templated nucleotide addition was plotted against the expression level for each miRNA with an average abundance over 10 reads per million (RPM). Error bar indicates the standard deviation ($n=3$). (C) miR-27a was ectopically expressed in HEK293T cells. Small RNAs from inputs or anti-AGO2-IP were subjected to deep sequencing. The percentages of canonical miR-27a, its tailed isomiRs and trimmed isomiRs relative to the total miR-27a reads were plotted.

A**B****Figure S2. An upstream adenosine requirement for miR-27a repression. Related to Figure 2.**

(A) Schematic representation of the pairing between miR-27a (top) and various target sequences (bottom). Non-templated U-tail is labeled with red circle. Yellow box indicates the adenosines upstream of target sequence. (B) Various renilla luciferase reporters were co-transfected with antagomirs (20 nM final concentration) of either anti-miR-27a or a control sequence into HeLa cells. Small RNAs were extracted and subject to Northern blotting. Endogenous miR-27a-3p was detected by probe-miR-27a.

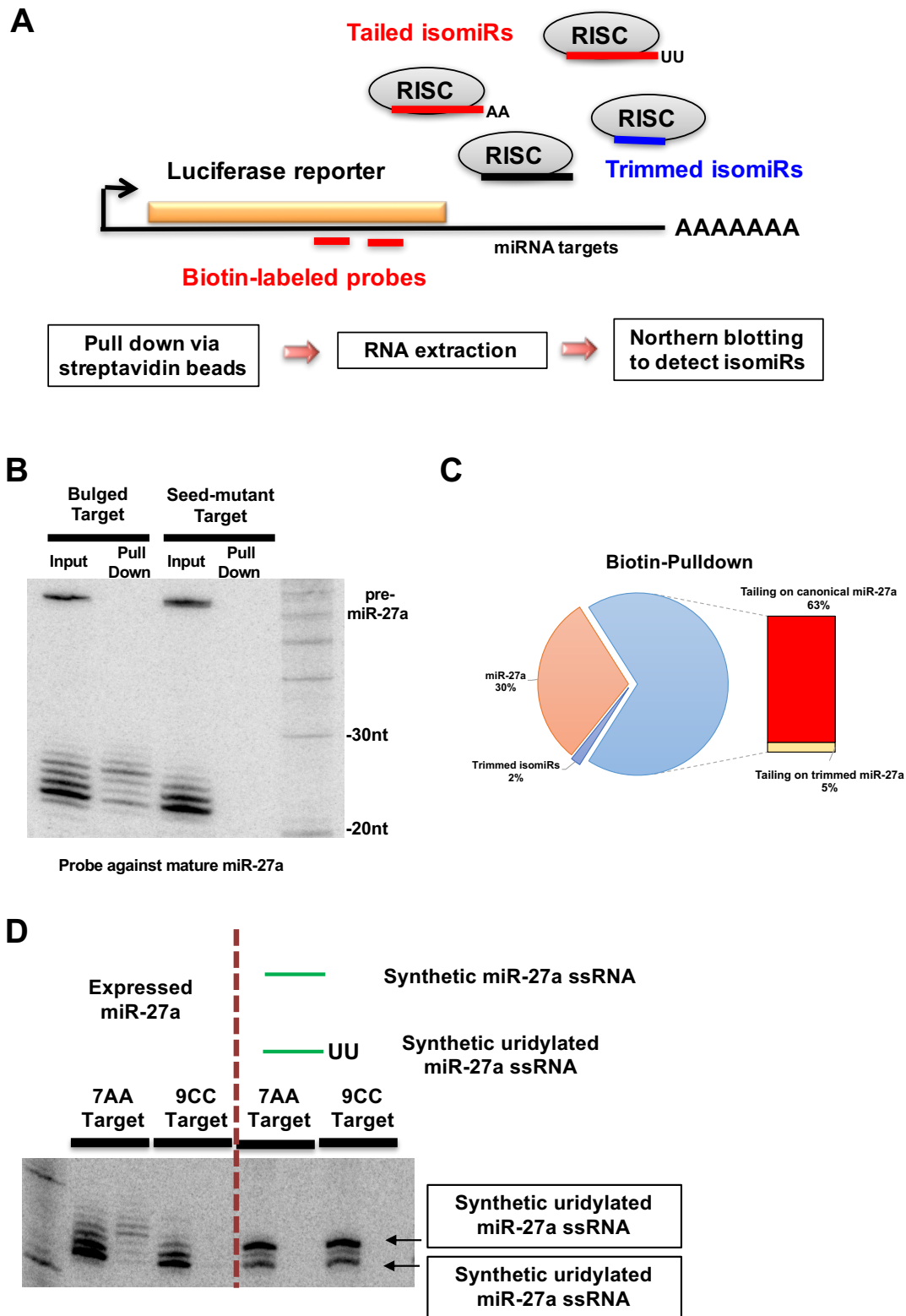


Figure S3. Uridylated miR-27a isomiRs repress non-canonical targets. Related to Figure 3.
(A) Schematic representation of the biotin-pull-down assay. **(B)** Biotin-pull-down assay was performed with either a functional target (Bulged) or a non-functional target (Seed-mutant). **(C)** Small RNAs from biotin-pull-downs of 7AA target were extracted and subjected to deep sequencing analysis. The percentage of canonical miR-27a, trimmed isomiRs and tailed isomiRs were shown in the pie chart. The tailed isomiRs were further divided into two groups: tailing on the canonical and tailing on the trimmed miR-27a. **(D)** single-stranded (ssRNA) miR-27a and uridylated miR-27a were mixed with cell lysates where either 7AA or 9CC targets were expressed. Biotin-pull-down analysis indicated that there were no associations. Biotin-pull-down assay with expressed miR-27a were performed in parallel and served as a positive control.

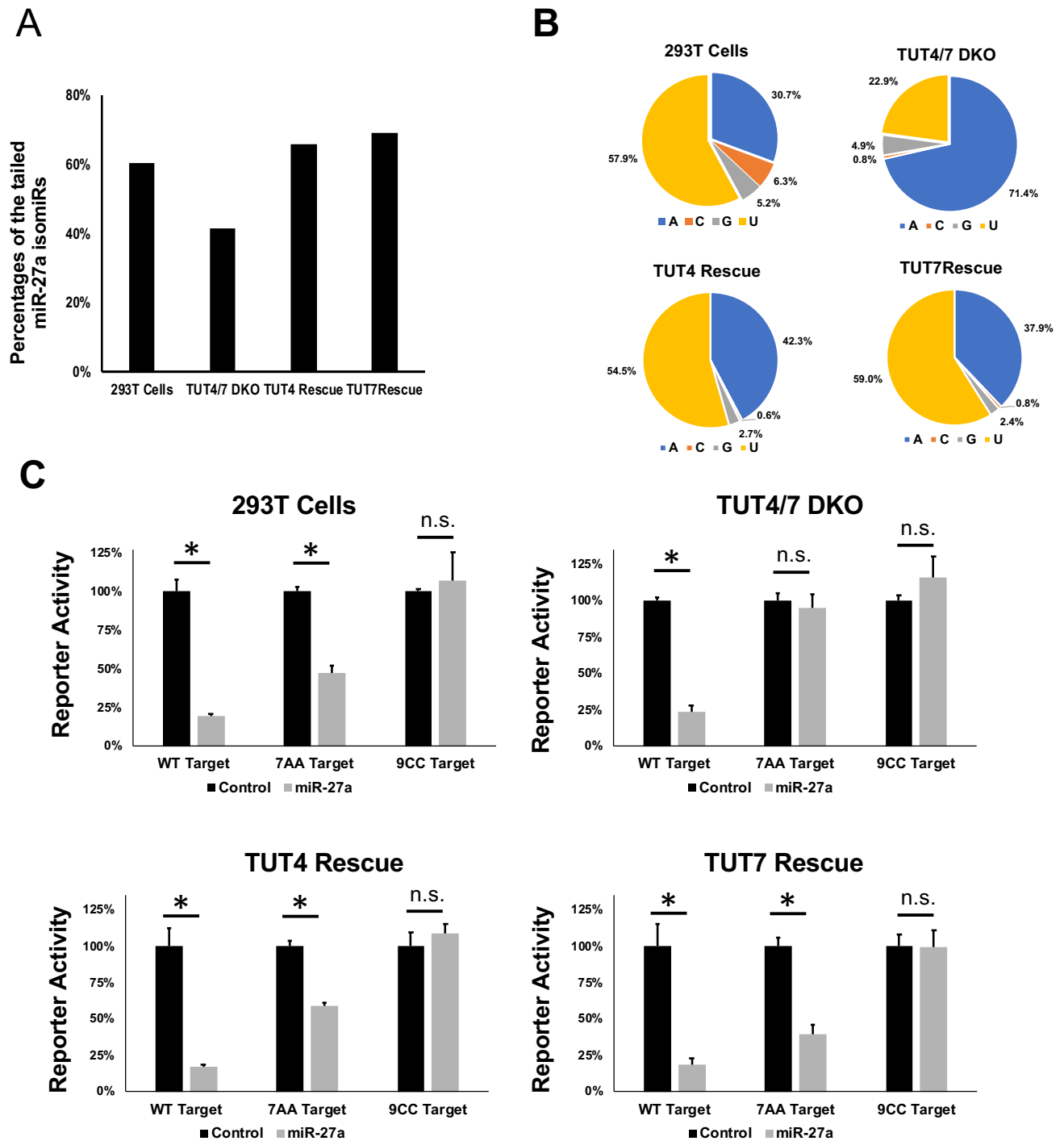


Figure S4. TUT4/TUT7-dependent repression of non-canonical targets. Related to Figure 4

(A) The percentages of tailed miR-27a isomiRs relative to all miR-27a reads and (B) Nucleotide compositions of non-templated tail of miR-27a isomiRs in either HEK293T or TUT4/7 DKO cells with or without TUT4/7 rescue were shown in the figure. (C) Various Dual-luciferase reporters were each co-expressed with miR-27a or a control miRNA in HEK293T cells and TUT4/7 DKO cells with or without TUT4/7 rescue. Dual-luciferase assays performed 48h post-transfection. Renilla luciferase activities were normalized with firefly luciferase, and the percentage of relative enzyme activity compared to the negative control (treated with the control non-target miRNA) was plotted. Error bars represent the standard deviation from three biological replicates. * $p < 0.001$, n.s. non-significant.

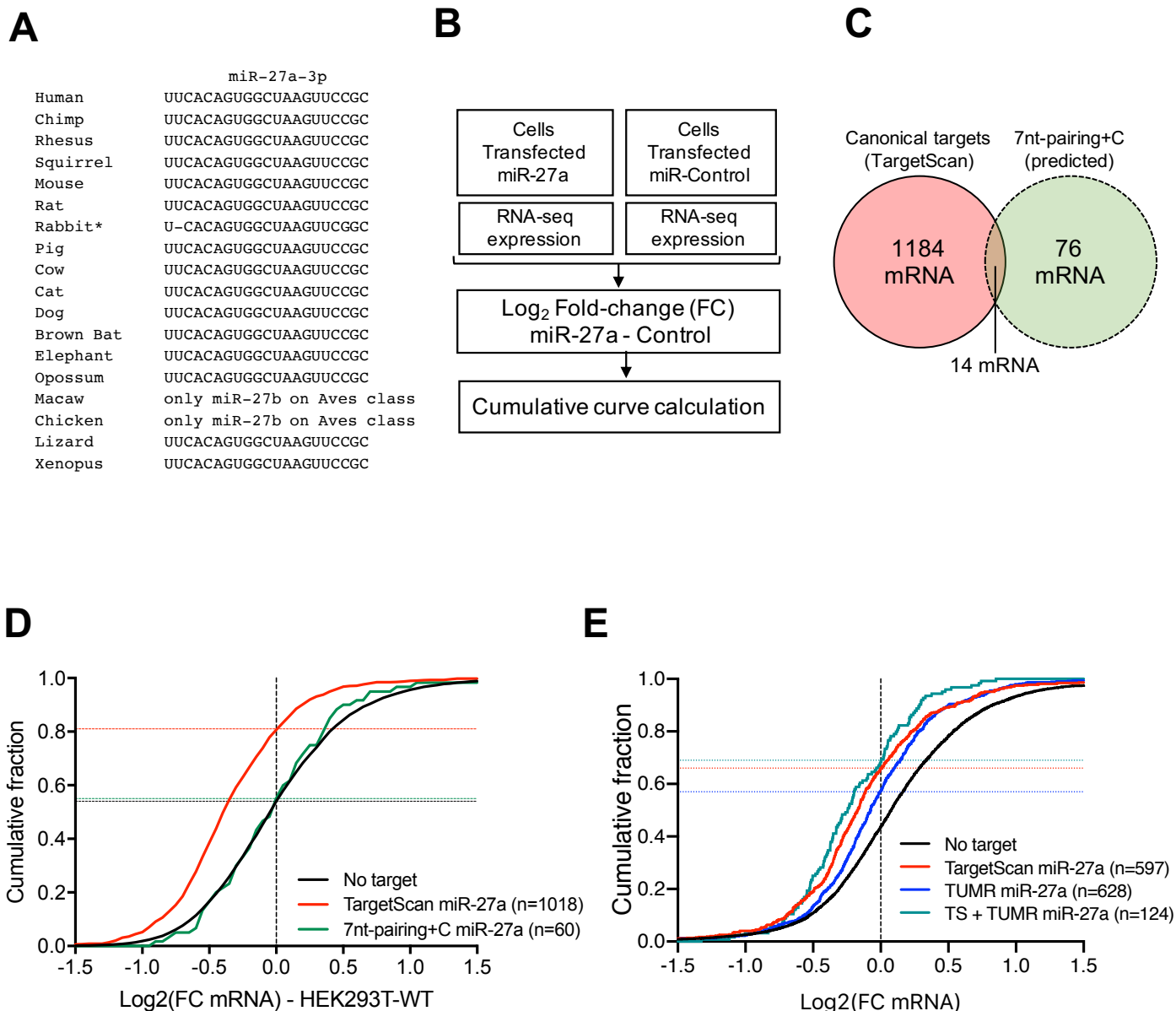


Figure S5. Uridylated miR-27a isomiRs repress a subset of endogenous mRNAs, Related to Figure 6.

(A) Sequence alignment of miR-27a orthologues in different species of vertebrates. (B) Diagram of the experimental and analysis pipeline used to obtain the Cumulative curves in Figures 6 and S5. (C) Venn diagram of canonical targets of miR-27a predicted by TargetScan (8mer, 7mer-A1, 7mer-m8) and conserved targets with “seedless” (7base-paired at 3’ region) plus C. (D) Cumulative curve comparing the effect of miR-27a canonical target sites (Adj. p-value<0.0001 vs. No target) and conserved targets with 7base-paired+C sites (Adj. p-value=n.s. non-significant vs. No target) on HEK293T cells. (E) Cumulative curve comparing the effect of miR-27a on mRNAs harboring TargetScan target sites (Adj. p-value<0.0001 vs. No target), TUMR target sites (Adj. p-value<0.0001 vs. No target) and both sites (Adj. p-value<0.0001) in mouse T cells. The number of genes analyzed in each group are in parentheses. The horizontal dash lines represent the fraction of repressed genes ($\text{Log}_2(\text{FC}) < 0$) in each group. Adjusted p-values were calculated using one-way ANOVA with multiple comparisons.

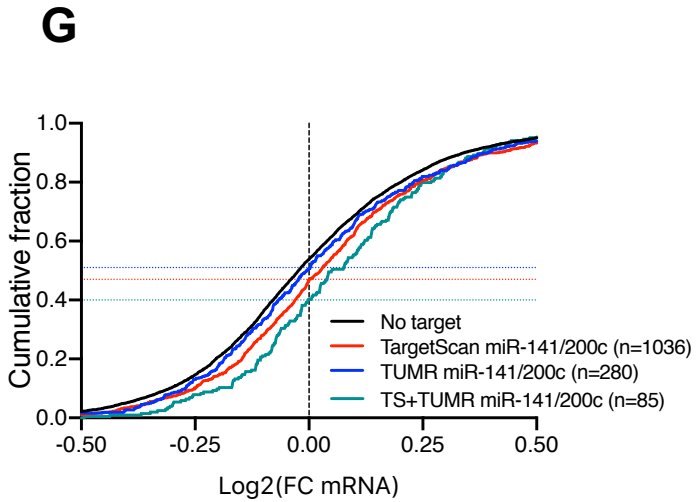
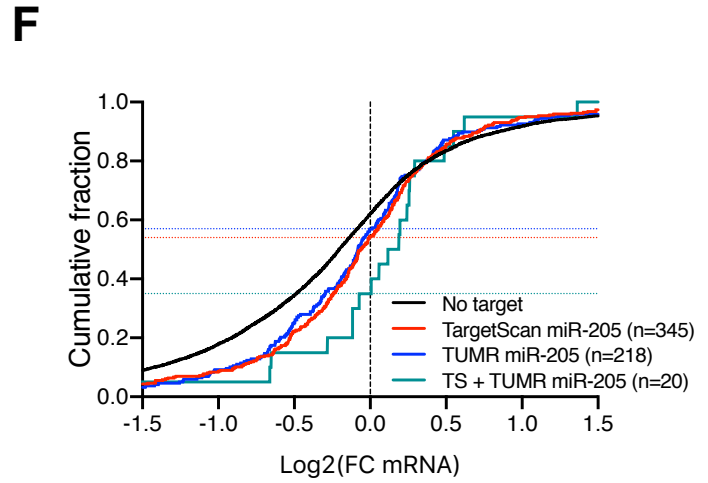
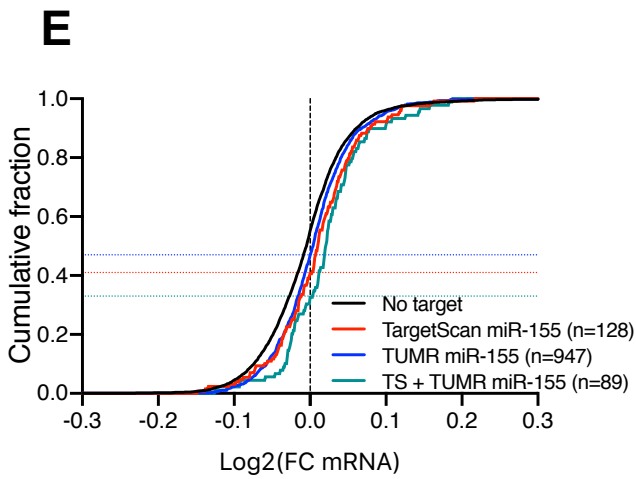
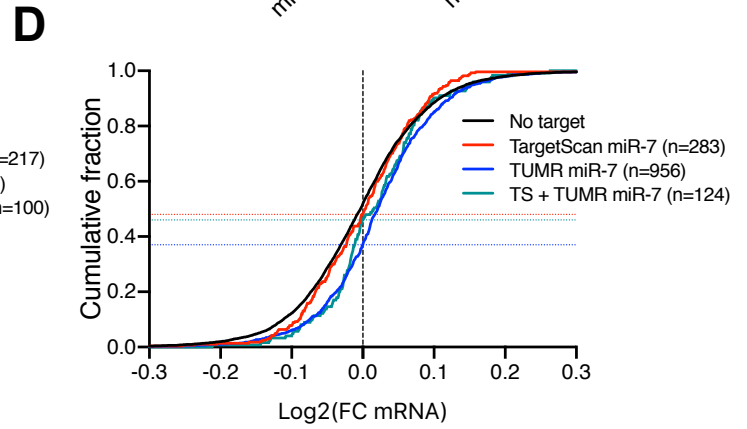
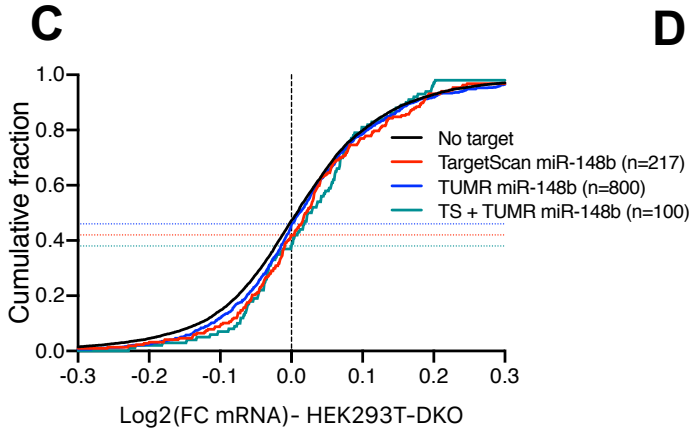
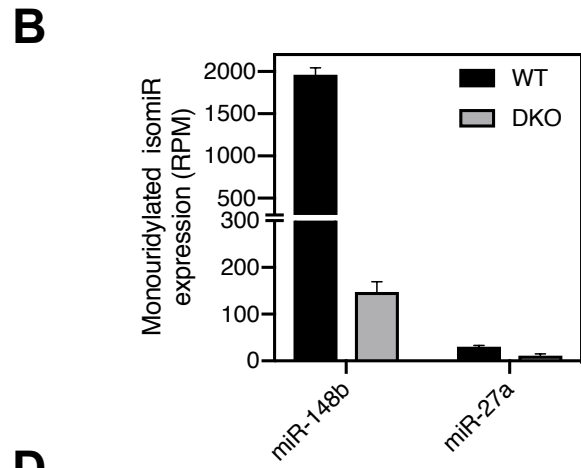
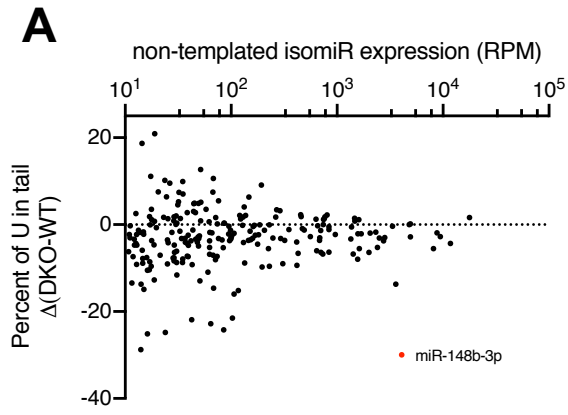


Figure S6. TUMR expands the target range of endogenous miRNAs, Related to Figure 7.

(A) Small RNAs extracted from WT HEK293T cells (n=3) and TUT4/7 DKO cells (n=4) were subjected to deep sequencing and the isomiR profiles compared. For each miRNA, the change of the “U” percentage in the tail upon TUT4/7 depletion was plotted against the isomiR expression level in HEK293T cells. **(B)** The average levels of mono-uridylylated miR-148b and miR-27a in WT HEK293T and TUT4/7 DKO cells. Error bar indicates the standard deviation. **(C)** Cumulative curve comparing the effect of miR-148b reduction on mRNAs containing TargetScan sites (vs. No target, non-significant), TUMR target sites (vs. No target, non-significant) and both sites (vs. No target, non-significant) in TUT4/7 DKO cells. **(D)** Cumulative curve comparing the effect of miR-7 reduction on mRNAs harboring TargetScan target sites (vs. No target, non-significant), TUMR target sites (Adj. p-value<0.0001 vs. No target) and both sites (Adj. p-value<0.0001) in mouse brain. **(E)** Cumulative curve comparing the effect of miR-155 depletion on mRNAs harboring TargetScan target sites (Adj. p-value<0.0001 vs. No target), TUMR target sites (Adj. p-value<0.0001 vs. No target) and both sites (Adj. p-value=0.0003) in mouse T cells. **(F)** Cumulative curve comparing the effect of miR-205 depletion on mRNAs harboring TargetScan target sites (Adj. p-value<0.0001 vs. No target), TUMR target sites (Adj. p-value=0.0038 vs. No target) and both sites (Adj. p-value=0.00165) in mouse mammary epithelial cells. **(G)** Cumulative curve comparing the effect of miR-141/200c depletion on mRNAs harboring TargetScan target sites (Adj. p-value<0.0001 vs. No target), TUMR target sites (Adj. p-value= 0.2712 vs. No target) and both sites (Adj. p-value=0.0003) in SK-BR-3 cells.

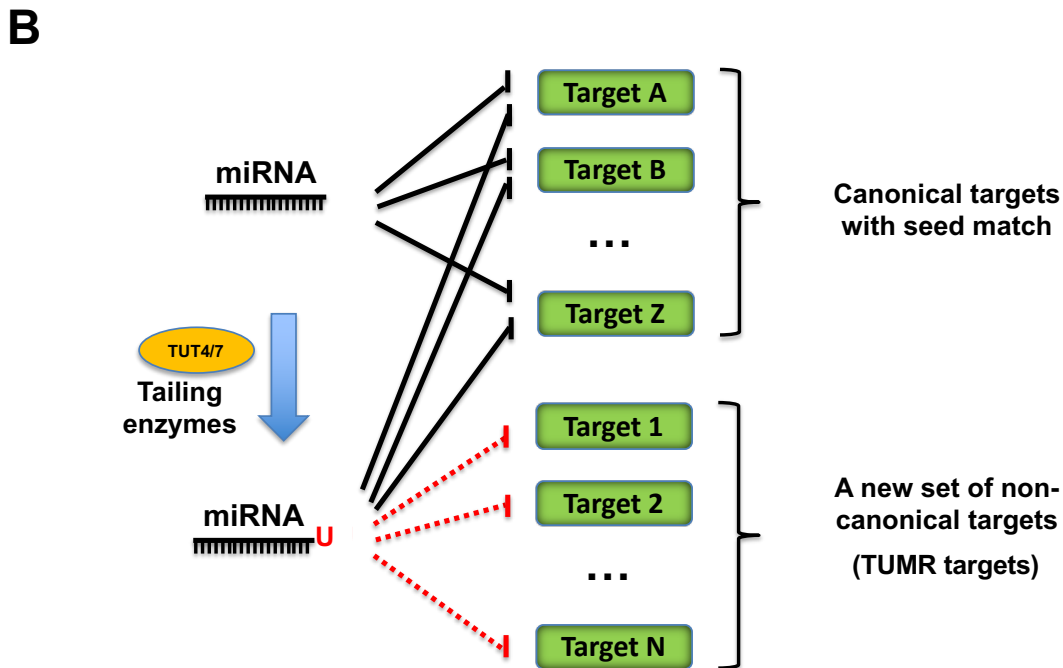
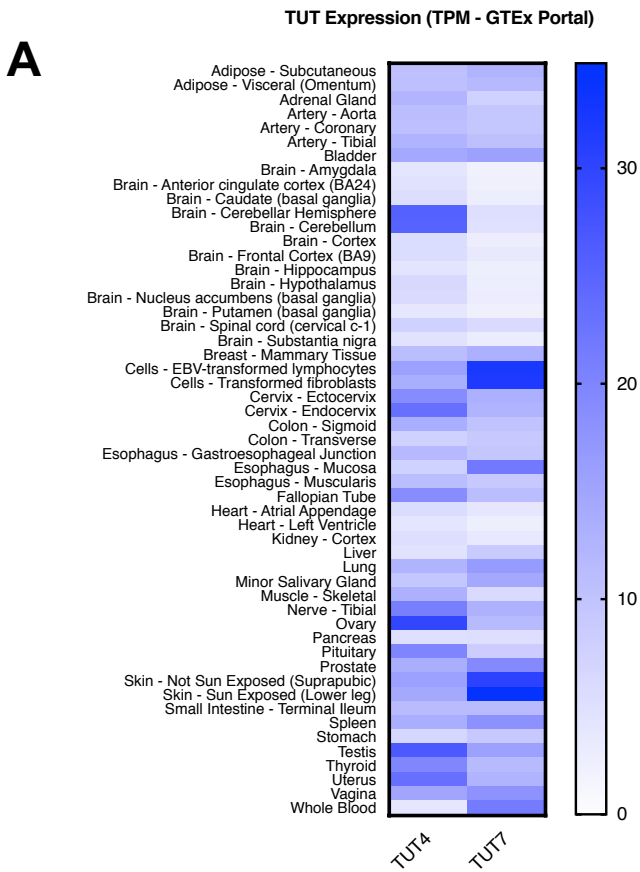


Figure 7. Proposed model of how uridylation expands miRNA target repertoire. Related to Figure 7.

(A) Expression levels of TUT4 and TUT7 are tissue-specific. Expression data (TPM, Transcripts per Million) was obtained from The Genotype-Tissue Expression Portal (GTEx February 2019) (Pangala et al., 2017) (B) Model for how uridylation expands miRNA target repertoire. Black solid lines: known canonical repression. Red dashed lines: Tail-U mediated repression (TUMR), which is dependent on TUT4/7 activities.